



## SHEARING RESISTANCE OF FRACTURES IN SATURATED PHRA WIHAN SANDSTONE

Pittawat Liapkrathok<sup>1</sup>, Supattra Khamrat<sup>2</sup>, Thanittha Thongprapha<sup>2</sup> and Kittitep Fuenkajorn<sup>3</sup>

<sup>1</sup>Student, Geomechanics Research Unit, Suranaree University of Technology, Thailand

<sup>2</sup>Researcher, Geomechanics Research Unit, Suranaree University of Technology, Thailand

<sup>3</sup>Professor, Geomechanics Research Unit, Suranaree University of Technology, Thailand

### บทคัดย่อ

การทดสอบกำลังเฉือนภายใต้ความเค้นในสามแกน ได้ถูกดำเนินการเพื่อประเมินผลกระทบของน้ำและความเค้นล้อมรอบต่อกำลังเฉือนสูงสุดและการขยายตัวของรอยแตกผิวขรุขระและรอยแตกผิวเรียบของหินทรายพระวิหาร โครงทดสอบในสามแกนได้นำมาใช้ให้แรงล้อมรอบแก่ตัวอย่างผันแปรอยู่ระหว่าง 1 ถึง 18 เมกะปาสกาล และความเร็วในการเฉือนผันแปรจาก  $1.15 \times 10^{-5}$  ถึง  $1.15 \times 10^{-2}$  มิลลิเมตรต่อวินาที ผลการทดสอบระบุว่าน้ำในรอยแตกส่งผลให้กำลังเฉือนสูงสุดและกำลังเฉือนคงเหลือของรอยแตกลดลง กำลังเฉือนสูงสุดของรอยแตกผิวเรียบมีแนวโน้มไม่ขึ้นกับความเร็วในการเฉือนและความอิ่มตัวด้วยน้ำ ที่ความเค้นล้อมรอบเดียวกัน กำลังเฉือนสูงสุด กำลังเฉือนคงเหลือ และอัตราการขยายตัวของรอยแตกผิวขรุขระมีค่าเพิ่มขึ้นเมื่อความเร็วในการเฉือนเพิ่มขึ้น พื้นที่ที่ถูกเฉือนเพิ่มขึ้นเมื่อความเค้นล้อมรอบเพิ่มขึ้นและเมื่อความเร็วในการเฉือนลดลง สมการเชิงประจักษ์ได้ถูกเสนอเพื่ออธิบายกำลังเฉือนสูงสุดและกำลังเฉือนคงเหลือของรอยแตกในหินทรายที่อิ่มตัวด้วยน้ำ สมการดังกล่าวสอบเทียบได้ดีกับผลการทดสอบและสามารถนำไปใช้คาดคะเนกำลังเฉือนของรอยแตกหินทรายที่อิ่มตัวด้วยน้ำภายใต้ความเค้นต่างๆ ในภาคสนาม

### ABSTRACT

Triaxial shear tests are performed to assess the effects of water saturation and confining pressure on shear strengths and dilations of tension-induced fractures and smooth saw-cut surfaces prepared in Phra Wihan sandstone. A polyaxial load frame is used to apply confining pressures between 1 and 18 MPa with displacement velocities ranging from  $1.15 \times 10^{-5}$  to  $1.15 \times 10^{-2}$  mm/s. The results indicate that water saturation of the rock can reduce the peak and residual shear strengths of the fractures. Shearing resistances of smooth saw-cut surfaces tend to be independent of the displacement velocity and water saturation. Under each confinement the peak and residual shear strengths and dilation rates of rough fractures increase with displacement velocities. The sheared-off areas increase when the confining pressure increases, and the displacement rate decreases. An empirical criterion that explicitly incorporates the effects of shear velocity is proposed to describe the peak and residual shear strengths of fractures in saturated sandstone. The criterion fits well to the test results, which may be used to predict the shear strengths of the saturated sandstone under in-situ condition.

**KEYWORDS:** Displacement Velocity, Shear Strength, Dilation, Rock Fracture

## 1. Introduction

Understanding of the frictional behavior of rock fractures is important for the prediction of natural geologic hazards (e.g., fault movements and landslides), and for the stability evaluation of geo-engineering structures (e.g., tunnels, mine openings, foundations and waste repositories). The friction of discontinuities in rock mass is one of the main factors governing the mechanical stability of underground excavations (e.g. [1-2]). The triaxial shear test method has been developed to simulate the frictional resistance of rock fractures under confinements. The cylindrical rock core containing an inclined fracture or weakness plane can be axially loaded in a triaxial pressure cell with a wide range of applied confining pressures. The normal stress at which the shear strengths are measured can be controlled by the applied axial stress and confining pressures [3-4].

Relevant factors influencing the shearing behavior of rock fractures have been identified and studied. These include, for example, scale effect [5], thermal loading [6], cyclic loading [7] and water pressure [8]. The effects of water saturation of the rock on the shearing behavior of its fractures have rarely been addressed and experimentally investigated. Such condition may occur in rock embankments around the reservoir during drawdown and along roadways that subjected to long period of rainfall. Even though the water in fractures can be drained out relatively quickly, the water in pore space of the rock hosting the fractures may influence the fracture shear strength. A criterion that can describe the shearing resistance of fractures in saturated rock has never been developed.

The objective of this study is to develop a fracture shear strength criterion that can explicitly incorporate the effects of water saturation, confining pressure and displacement velocity. The task involves performing triaxial shear tests to obtain the strengths and dilations of fractures in saturated sandstone under confining pressures up to 18 MPa. Tension-induced fractures and smooth saw-cut surfaces are prepared and tested in the sandstone specimens. Under each confinement the fractures are sheared with constant displacement velocities ranging from  $1.15 \times 10^{-2}$  to  $1.15 \times 10^{-5}$  mm/s. The joint roughness coefficients (JRC) are determined prior to and after shearing.

## 2. Sample Samples

The rock sample used in this study is the Phra Wihan sandstone. It is fine-grained comprising 72% quartz (0.2-0.8 mm), 20% feldspar (0.1-0.8 mm), 3% mica (0.1-0.3 mm), 3% rock fragment (0.5-2 mm), and 2% other (0.5-1 mm) [9]. The specimen density is averaged as  $2.35 \pm 0.1$  g/cc. The Phra Wihan sandstone is largely exposed in the northeast of Thailand where it is the host rock to several tunnel roadways and railways, power plants, reservoir and dam foundations.

For the triaxial shear testing the specimens are prepared to obtain rectangular blocks with nominal dimensions of  $50 \times 50 \times 87$  mm<sup>3</sup>. Two types of fractures are artificially made in the laboratory: tension-induced fractures and smooth saw-cut surfaces. They have nominal areas of  $50 \times 100$  mm<sup>2</sup>. A line load is applied to obtain a tension-induced fracture diagonally across the rock block, as shown in Figure 1(a). The smooth fractures are made by using a universal masonry saw. The normal to the fracture plane makes an angle ( $\beta$ ) of  $59.1^\circ$  with the specimen vertical axis. The tension-induced fractures are clean and well mated. The asperity amplitudes are measured from the laser-scanned profiles along the shear direction. The readings are made to the nearest

0.01 mm. Figure 1(b) shows an example of laser scanned image. The maximum amplitudes are used to determine the joint roughness coefficients (JRC) of each fracture based on the Barton's chart [10]. The means and standard deviations of the JRC's are  $10 \pm 0.5$ . To saturate the rock specimens, they are submerged in water filled vacuum chamber under the negative pressure of 0.1 MPa. The vacuum chamber is connected to a vacuum pump capable of inducing negative 1 atm. Their weights are measured every two hours. This pressure treatment is repeated until the specimen weight remained unchanged. The water contents under saturation of the Phra Wihan sandstone specimens are about 5%.

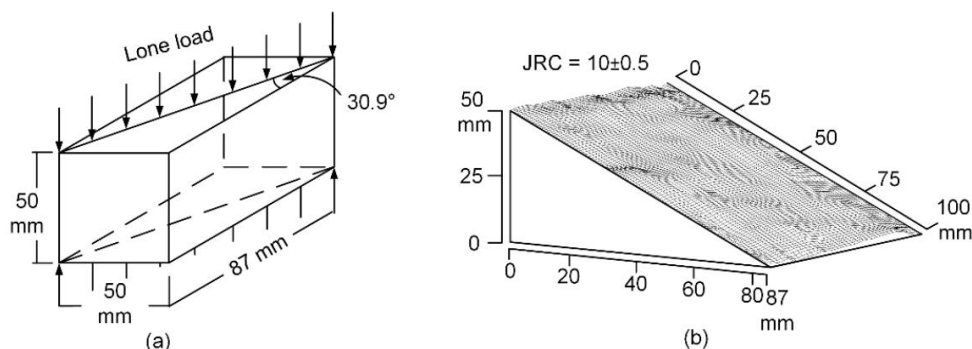


**Figure 1** Line load applied to obtain tension-induced fracture in rock specimen (a), and example of fracture image obtained from laser scanning (b)

### 3. Test Apparatus and Method

A polyaxial load frame [11] is used to apply constant and uniform lateral stresses (confining pressures,  $\sigma_2 = \sigma_3$ ) and vertical (axial -  $\sigma_1$ ) stress to the block specimen. Figure 2 shows the directions of the applied stresses with respect to fracture orientation. The confining pressures are maintained constant at 1, 3, 7, 12 and 18 MPa for tension-induced fractures, and at 3, 7 and 12 MPa for smooth saw-cut surfaces.

The shear stress ( $\tau$ ) and its corresponding normal stress ( $\sigma_n$ ) on the fracture can be determined from the applied principal stresses ( $\sigma_1$  and  $\sigma_3$ ) as follows [4, 12]:

$$\tau = \frac{1}{2}(\sigma_1 - \sigma_3) \cdot \sin 2\beta \quad (1)$$

$$\sigma_n = \frac{1}{2}(\sigma_1 + \sigma_3) + \frac{1}{2}(\sigma_1 - \sigma_3) \cdot \cos 2\beta \quad (2)$$

where  $\beta$  is the angle between  $\sigma_1$  and  $\sigma_n$  axes. The shear and normal (dilation) displacements ( $d_s$  and  $d_n$ ) can also be calculated from the vertical and lateral displacements ( $d_1$  and  $d_3$ ) as:

$$d_s = d_1 / \sin \beta \quad (3)$$

$$d_n = (d_{3,m} - d_{3,c}) \cdot \sin \beta \quad (4)$$

$$d_{3,c} = \tan(90 - \beta) \cdot d_1 \quad (5)$$

where  $d_{3,m}$  is the total lateral displacement measured during the test, and  $d_{3,c}$  are the calculated lateral displacement induced by the vertical displacement on the incline fracture plane. Using Equation (3) the shear displacement velocities ( $\dot{d}_s/\dot{d}$ ) that are equivalent

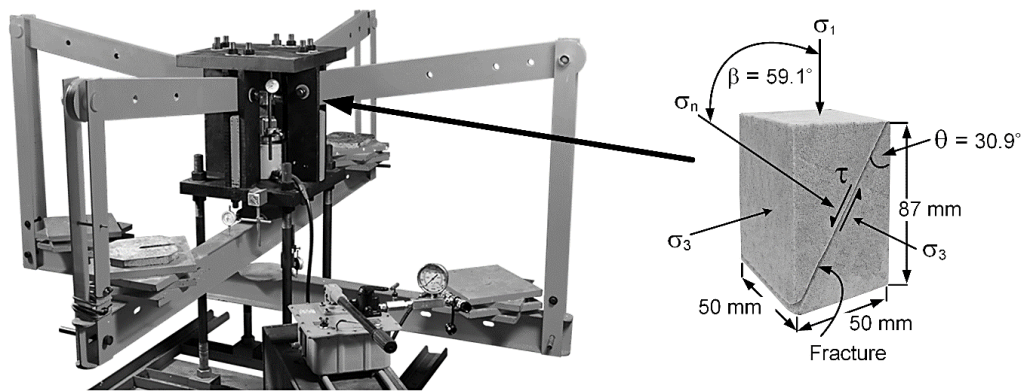


**Figure 2** Polyaxial load frame and directions of applied stresses

to the applied axial displacement velocities ( $\dot{d}_1/\dot{d}$ ) of  $10^{-5}$ ,  $10^{-4}$ ,  $10^{-3}$  and  $10^{-2}$  mm/s are calculated as  $1.15 \times 10^{-5}$ ,  $1.15 \times 10^{-4}$ ,  $1.15 \times 10^{-3}$  and  $1.15 \times 10^{-2}$  mm/s.

#### 4. Test Results

The shear stress-displacement ( $\tau$ - $d_s$ ) curves obtained under all displacement velocities are shown in Figure 3. Under each confining stress ( $\sigma_3$ ), the differences between the peak and residual stresses notably reduced when the fractures are subjected to lower shear velocities. The major principal stresses for the peak ( $\sigma_{1,p}$ ) and residual ( $\sigma_{1,r}$ ) increase non-linearly with displacement velocities, as shown in Figure 4. Using Equations (1) and (2) the peak and residual shear strengths and their corresponding normal stresses can be calculated. The shear and normal (dilation) displacements of the tested fractures can be calculated using Equations (3) and (4).

Figure 5 shows that the dilation rates increase with the displacement velocity. The dilation of fractures in saturated sandstone is lower than those in dry sandstone (obtained from Klepeck et al. [13]). This may be due to the fact that rock asperities under saturation can be sheared-off more easily than those under dry condition. Table 1 shows examples of post-test fractures obtained under the highest and lowest displacement velocities and confining stresses. The light areas on the fracture

surfaces represent the sheared-off asperities. This visual observation supports the previous results that higher confining pressure and lower shear velocities can reduce fracture dilation, and hence enhances the sheared-off areas on the fracture.

## 5. Empirical Criterion

An empirical criterion is proposed to represent the fracture shear strengths as a function of normal stress, as follows [13]:

$$\tau = \alpha \cdot \sigma_n^\lambda \quad (6)$$

where  $\alpha$  and  $\lambda$  are empirical parameters, depending on rock types. Regression analyses are performed on Equation (6). Good correlations are obtained ( $R^2 \geq 0.9$ ). The parameters  $\alpha$  and  $\lambda$  determined for each shear velocity are summarized in Table 2.

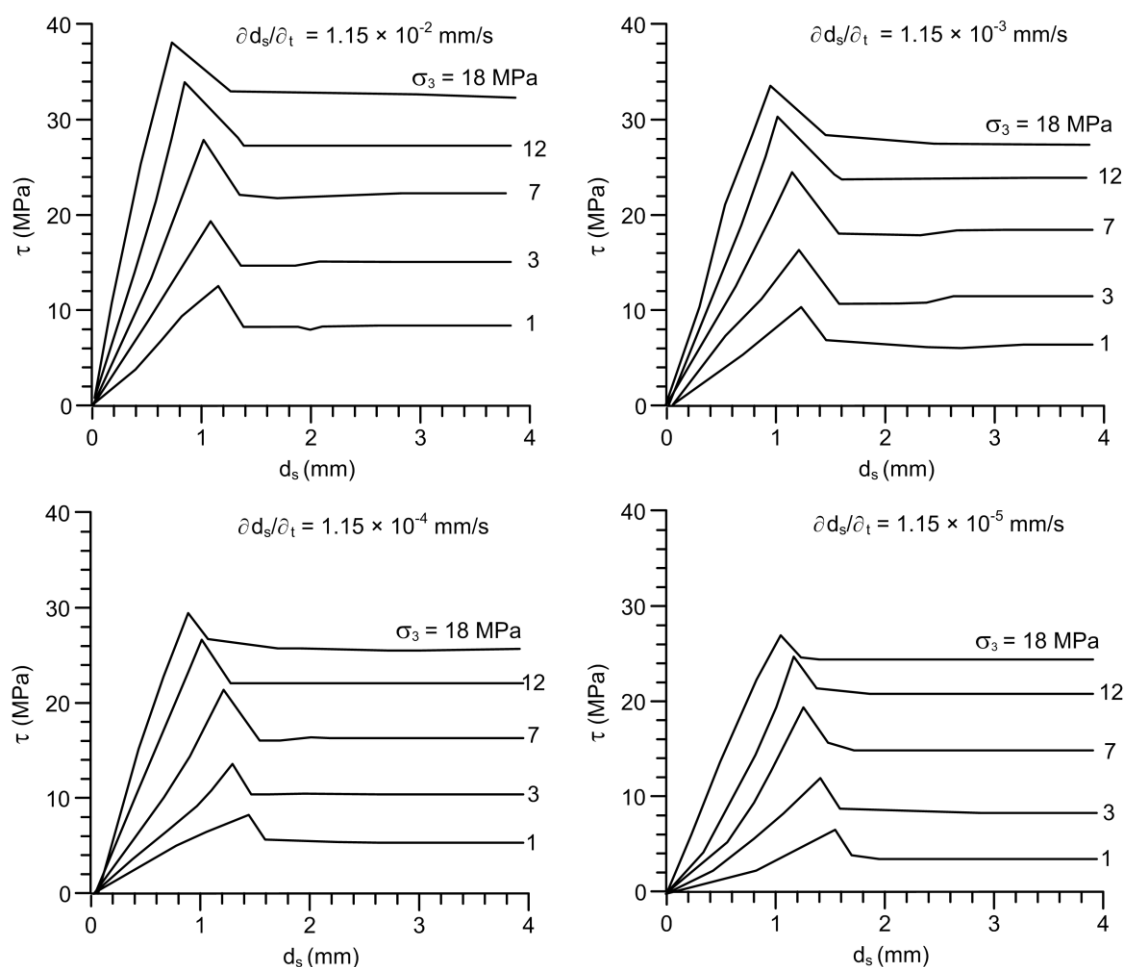
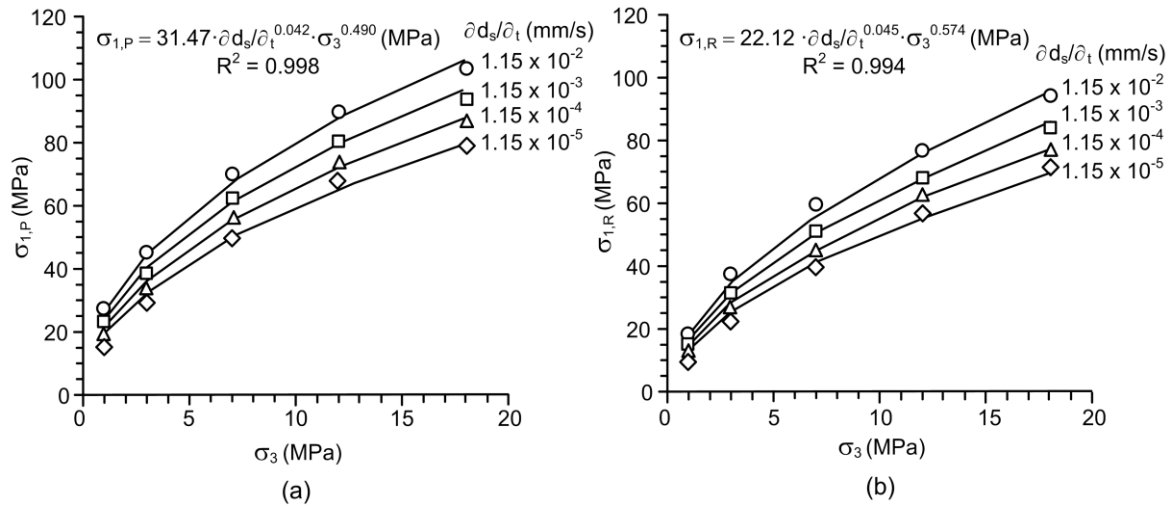
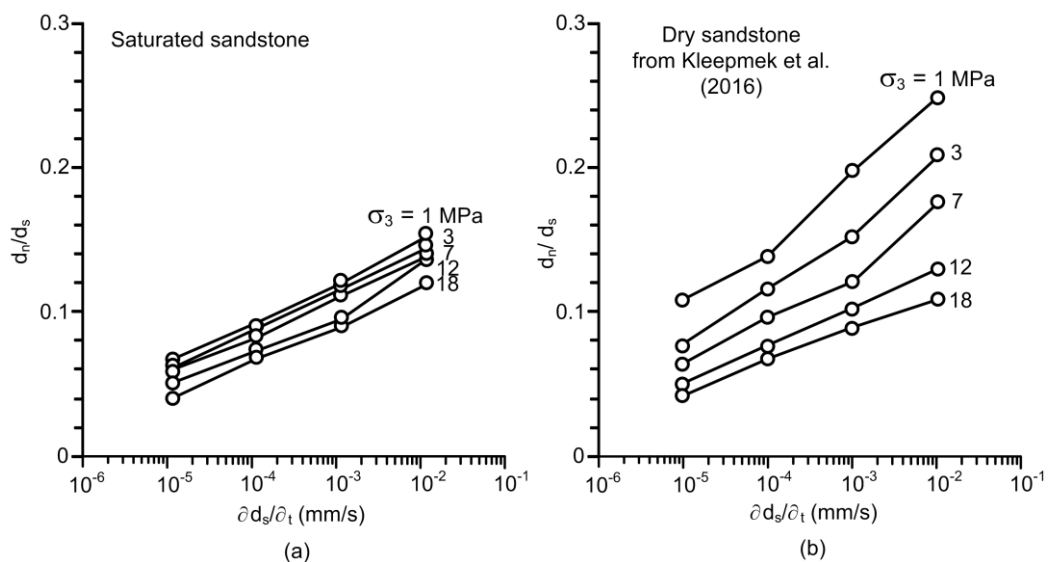


Figure 3 Shear stresses ( $\tau$ ) as a function of shear displacement ( $\partial d_s / \partial t$ )

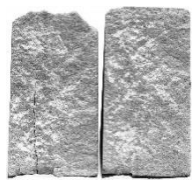
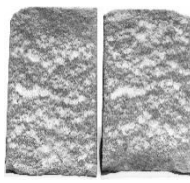
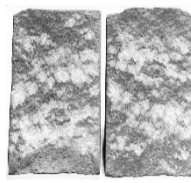
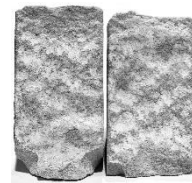
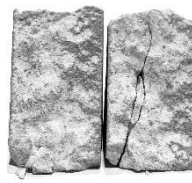
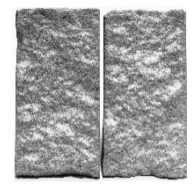
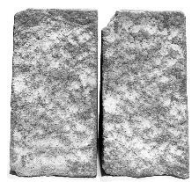
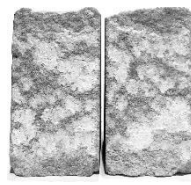
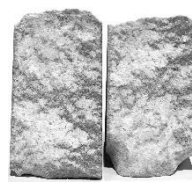
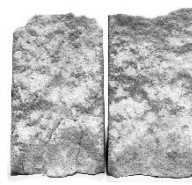


**Figure 4** Major principal stresses at peak,  $\sigma_{1,P}$  (a) and at residual,  $\sigma_{1,R}$  (b) as a function of confining stresses ( $\sigma_3$ )



**Figure 5** Dilation rates ( $d_n / d_s$ ) as a function of the shear velocity ( $\partial d_s / \partial t$ ) for saturated (a) and dry (b) sandstones

**Table 1** Some post-test fractures

$\dot{\alpha}_s/\dot{\alpha}$ (mm/s)	$\sigma_s$ (MPa)				
	1	3	7	12	18
$1.15 \times 10^{-2}$					
$1.15 \times 10^{-5}$					

**Table 2** Empirical parameters. Numbers in brackets indicate parameters obtained under dry condition by Kleepmek et al. [13]

$\dot{\alpha}_s/\dot{\alpha}$ (mm/s)	Peak		Residual	
	$\alpha$	$\lambda$	$\alpha$	$\lambda$
$1.15 \times 10^{-2}$	3.05 (3.31)	0.686 (0.700)	2.67 (2.74)	0.722 (0.721)
$1.15 \times 10^{-3}$	2.81 (3.10)	0.686 (0.700)	2.23 (2.54)	0.722 (0.721)
$1.15 \times 10^{-4}$	2.64 (2.90)	0.686 (0.700)	2.16 (2.36)	0.722 (0.721)
$1.15 \times 10^{-5}$	2.54 (2.71)	0.686 (0.700)	1.78 (2.18)	0.722 (0.721)

The parameter  $\lambda$  tends to be independent of the shear velocity for both saturated condition (obtained in this study) and dry condition (obtained by Kleepmek et al. [13]). It probably relates to the fracture roughness. For smooth saw-cut surface  $\lambda$  would be equal to 1.0. The parameter  $\alpha$  for both saturated and dry conditions increases with shear velocity ( $\partial \dot{\alpha}_s / \partial t$ ), which can be best represented by:

$$\alpha = \eta \dot{\alpha}_s^\omega \quad (7)$$

where  $\eta$  and  $\omega$  are empirical constants. Their numerical values are given in Figure 6. They are compared with those obtained by Kleepmek et al. [13] who conduct the same experiment on dry Phra Wihan sandstone. For both peak and residual the parameter  $\alpha$  for the saturated sandstones is lower than those of the dry one. For smooth saw-cut surface ( $\lambda = 1.0$ )  $\alpha$  is equal to  $\tan \phi_s$ , and is independent of the shear velocity. This means that  $\alpha$  is also dependent of fracture roughness, as evidenced by that  $\alpha$ 's for the peak shear strengths are higher than those for the residual shear strengths.

Substituting Equation (7) into Equation (6) the fracture shear strength criterion that considers the shear velocity effect can be obtained. Figure 7 compares the proposed criterion with the peak and residual shear strength results. The upper bound of the shear strengths is defined by the angle  $\beta$  which is maintained constant at 59.1 degrees. The lower bound is defined by the basic friction angle ( $\phi_b$ ) obtained from the smooth saw-cut surfaces testing.

## 6. Discussions and Conclusions

The test results clearly show that the water saturation of the sandstone can reduce its fracture shear strengths. The fracture dilations measured prior to and after the peak strengths significantly decrease with increasing confining pressures and decreasing displacement velocities. This is supported by the visual observations and the JRC measurements of the post-test fractures that

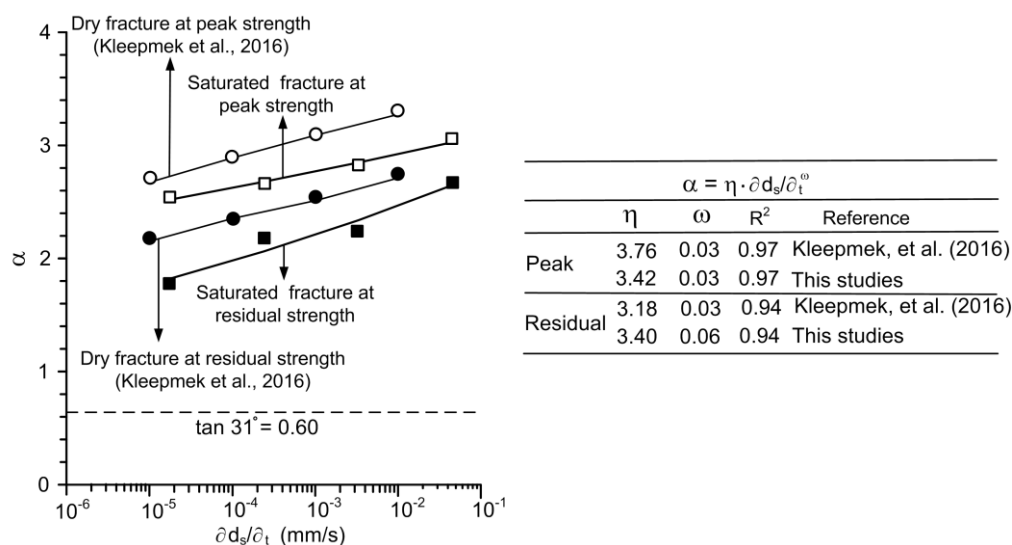


Figure 6 Parameter  $\alpha$  as a function of shear velocity

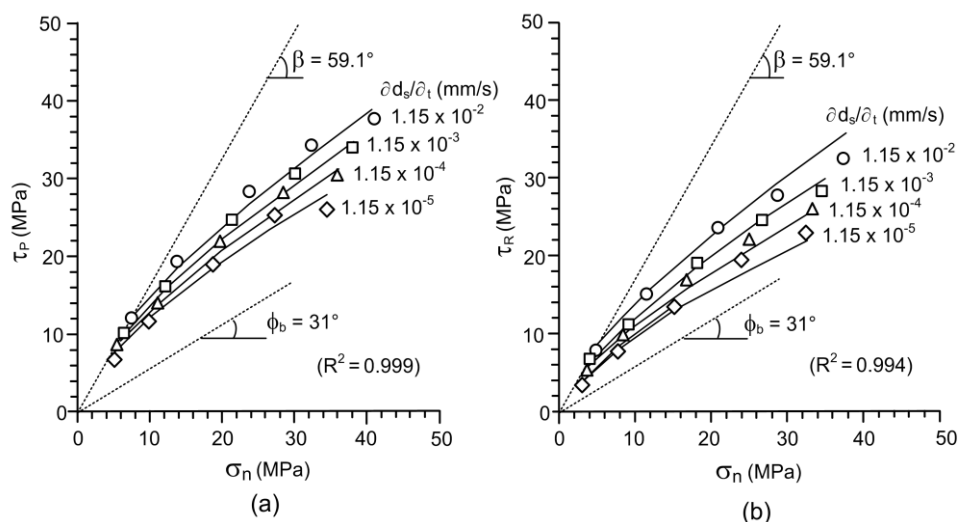


Figure 7 Comparison empirical criterion with test data for peak,  $\tau_p$  (a) and residual,  $\tau_r$  (b) shear strengths



the reduction of the shear velocity notably increases the sheared-off areas, particularly when the fractures are under high confining pressures. The  $\tau$ - $\sigma_n$  curves obtained under saturated condition tend to be lower than those obtained under dry condition by Kleepmek et al. (2016), as suggested by the parameter  $\alpha$  given in Figure 6. This is due to the effect of pore pressures particularly under high loading rates. Under low loading rates the pore water is allowed to drain from the specimens, and hence the effect of pore pressure becomes lower. The effect of water saturation also acts more under high confining pressures. It tends to be equally pronounced for all displacement velocities used in this test. This agrees reasonably well with the test results obtained by Khamrat et al. [14] who found that the compressive strengths of the saturated Phra Wihan sandstone intact specimens were lower than those of the dry ones. The water saturation has no effect on the smooth saw-cut fracture. The basic friction angle obtained under saturation obtained here is similar to that obtained under dry condition by Kleepmek et al. [13]. The parameter  $\alpha$  would increase with increasing fracture roughness, as suggested by that the higher  $\alpha$  is obtained under higher loading rate. For smooth fracture  $\alpha$  will equal to  $\tan\phi$  or about 0.601 for the tested sandstone. The parameter  $\lambda$  represents the non-linearity of the  $\tau$ - $\sigma_n$  curve. It would relate to the strength and roughness of the fractures.

It is recognized that increasing the number of the specimens under each confining stress and shear rate would statistically enhance the reliability of the test results and the predictability of the proposed strength criterion. Nevertheless, the results are adequately reliable, the measurement data conform reasonably well across the ranges of the test parameters (loading rates and confining stresses). Even though more samples are tested, they will not change the main conclusions drawn from the study. The results show definite trend in terms of the shear strengths as a function of normal stress for all shear velocities. The proposed empirical criterion also well fit to the test data as evidenced by the good correlation coefficients ( $R^2 > 0.9$ ). Equations (6) and (7) can be used as a strength criterion to assess the stability of sandstone slope embankment under saturation. This would give more conservative results, as compared to those obtained by using the criterion derived from dry condition testing.

### Acknowledgements

This study is funded by Suranaree University of Technology and by the Higher Education Promotion and National Research University of Thailand. Permission to publish this paper is gratefully acknowledged.

### References

- [1] Hoek, E. and Brown, E. T. *Underground Excavations in Rock*. Institution of Mining and Metallurgy: London, 1980.
- [2] Brady, B. H. G. and Brown, E. T. *Rock Mechanics for Underground Mining*. Springer: Netherlands, 2006.
- [3] Barton, N. The shear strength of rock and rock joint. *International Journal of Rock Mechanics and Mining Sciences and Geomechanics*, 1976, 13 (9), pp. 255-279.
- [4] Jaeger, J. C. et al. *Fundamentals of Rock Mechanics*. Blackwell Publishing: Malden, 2007.
- [5] Bandis, S. et al. Experimental studies of scale effects on the shear behaviour of rock joints. *International Journal of Rock Mechanics and Mining Sciences and Geomechanics*, 1981, 18 (1), pp. 1-21.
- [6] Stesky, R. M. et al. Friction in faulted rock at high temperature and pressure. *Tectonophysics*, 1974, 23 (1-2), pp. 177-203.

- 
- [7] Kamonphet, T. *et al.* Effects of cyclic shear loads on strength, stiffness and dilation of rock fractures. *Songklanakarin Journal of Science and Technology*, 2015, 37 (6), pp. 683-690.
  - [8] Stesky, R. M. Rock friction-effect of confining pressure, temperature and pore pressure. *Pure and Applied Geophysics*, 1978, 116 (4), pp. 690-704.
  - [9] Boonsener, M. and Sonpiron, K. Correlation of tertiary rocks in northeast, Thailand. *Proceeding of International Conference on Stratigraphy and Tectonic Evolution of Southeast Asia and the South Pacific*, 1997, pp. 656-661.
  - [10] Barton, N. Characterizing rock masses to improve excavation design. *Proceeding of 4th Congress IAEG*, 1982.
  - [11] Fuenkajorn, K. and Kenkhunthod, N. Influence of loading rate on deformability and compressive strength of three Thai sandstones. *Geotechnical and Geological Engineering*, 2010, 28 (5), pp. 707-715.
  - [12] Barton, N. Shear strength criteria for rock, rock joints, rockfill and rock masses: Problems and some solutions. *Journal of Rock Mechanics and Geotechnical Engineering*, 2013, 5 (4), pp. 249-261.
  - [13] Kleepmek, M. *et al* Displacement velocity effects on rock fracture shear strengths. *Journal of Structural Geology*, 2016, 90, pp. 48-60.
  - [14] Khamrat, S. *et al* Pore pressure effects on strength and elasticity of ornamental stones. *Science Asia*, 2016, 42 (2), pp. 121-135.